International Journal of Mechanical, Industrial and Aerospace Sciences
ISSN: 2517-9950
Vol:3, No:11, 2009

Design and Trajectory Planning of Bipedal Walking Robot with Minimum Sufficient Actuation System

H. Siswoyo Jo, N. Mir-Nasiri, and E. Jayamani

***Abstract*—**This paper presents a new type of mechanism and trajectory planning strategy for bipedal walking robot. The newly designed mechanism is able to improve the performance of bipedal walking robot in terms of energy efficiency and weight reduction by utilizing minimum number of actuators. The usage of parallelogram mechanism eliminates the needs of having an extra actuator at the knee joint. This mechanism works together with the joint space trajectory planning in order to realize straight legged walking which cannot be achieved by conventional inverse kinematics trajectory planning due to the singularity. The effectiveness of the proposed strategy is confirmed by computer simulation results.

***Keywords*—**Bipedal robot, Energy efficiency, Straight legged walking, Trajectory planning.

I. Introduction

NOWADAYS, the development of robotics system to assist and replace human in various tasks is continuously growing. But, most of the existing robots work in a restricted environment such as assembly lines and product inspection.

In order for a robot to be able to replace human completely, one of the criteria is to have a similar physical structure with human. This will enable the robot to work and directly adapt into human environment.

Locomotion style is the most essential characteristic that the robot needs to replicate from human. Throughout these forty years, researchers have been discussing about bipedal locomotion especially in the part related to walking pattern and stability analysis [1-10]. Over the years, many bipeds are built by public research laboratories, universities and major companies. Honda R&D Co.Ltd. [6,7] has come out with their famous ASIMO which is a human scale humanoid robot. Waseda University [8-10] who pioneered the research in bipedal robot has also comes out with WL-12RV walking robot and WABIAN humanoid robot.

However, not many existing bipedal robots are equivalent to human in terms of the walking gait. The most obvious difference is due to the fact that they can't perform straight legged walking because of singularity problems in the inverse kinematics calculation. Besides producing a more natural walking pattern, straight legged walking will also help to improve its energy efficiency since the torque required to supports the body weight become small at knee joints.

To realize straight legged walking, some researchers have come out with different strategies. R.Kurazume et al [11] proposed a methodology for generating a straight legged walking pattern for a biped robot utilizing up-and-down motion of an upper body. On the other hand, Y.Ogura et al [12] proposed a technique to avoid singularity by adding roll motion to the waist.

This paper introduces a new type of mechanism for bipedal leg and a different approach of controlling the mechanism directly at the joint coordinate in order to achieve straight legged walking. This new type of mechanism is designed to employ minimum number of actuators which lead to a lightweight and energy efficient walking robot.

Details of the design are presented as follows. Section II discuss about the mechanical components and structure, section III discuss about trajectory planning strategy. In section IV, computer simulation results are presented followed by conclusion of work in section V.

II. Mechanical Structure of Robot Legs

The mechanical system of the robot has been divided into two separate subsystems:

- Robot driving subsystem (robot legs)
- Robot balancing mechanism

This paper describes only the robot leg structure and its trajectory planning.

The robot leg structure is shown in Fig. 1.

H.Siswoyo is with School of Engineering and Science, Swinburne University of Technology (Sarawak Campus), Kuching 93350, Malaysia (e-mail: hsiswoyo@ swinburne.edu.my).

N. Mir-Nasiri, is with School of Engineering and Science, Swinburne University of Technology (Sarawak Campus), Kuching 93350, Malaysia (e-mail: nnasiri@ swinburne.edu.my).

E. Jayamani is with School of Engineering and Science, Swinburne University of Technology (Sarawak Campus), Kuching 93350, Malaysia (e-mail: ejayamani@ swinburne.edu.my).

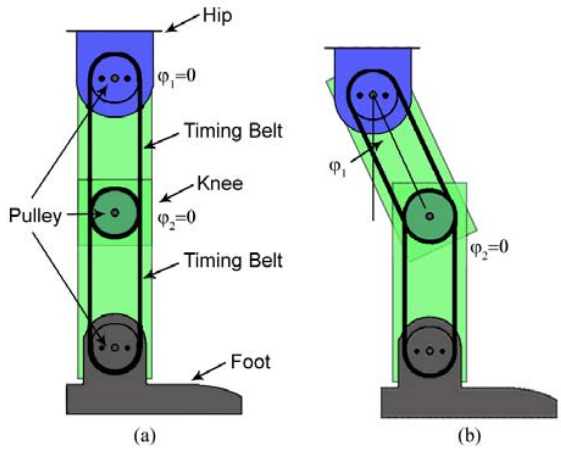

Fig. 1 Simplified structure of the leg

The main components of the legs are timing belts and pulley system that work as a parallelogram mechanism. The advantages of selecting parallelogram mechanism are:

- To decouple the motion of the upper leg from the lower leg
- To maintain the foot plane level always parallel to the ground while the robot moves

Fig. 1(a) shows that when upper and lower sections of the leg are both vertical, the actuation angles are initialized to zero. Fig. 1(b) shows the upper section of the leg after it has been actuated. However, lower section of the leg still maintains its vertical position (φ_2=0) and foot plane remains horizontal. This structure still allows adding certain controllable degree of freedom to the ankle to accommodate some irregularities of the ground. The advantage of this structure is that the motion can be performed without necessity of having actuators at the ankle joint; hence only four actuators are required to accommodate walking pattern.

III. Trajectory Planning

A. Classification of angular boundary conditions for different leg postures

The entire trajectory planning for the robot leg motion in Cartesian space is achieved only by controlling the motors shaft motions in the Joint space. Matching of the parameters in Joint and Cartesian spaces is achieved by careful selection of boundary conditions for the joint space control and proper timing. This will provide smooth transition from one section of the time into another one.

The joint space trajectories are designed to fulfill the following boundary conditions for a joint motion during time $0<t<t_f$

$$\text{when } t=0, \varphi(0)=\varphi_i\,;\dot{\varphi}(0)=0\,;\ddot{\varphi}(0)=0$$
$$\text{when } t=t_f, \varphi(t_f)=\varphi_f\,;\dot{\varphi}(t_f)=0\,;\ddot{\varphi}(t_f)=0$$

φ_i - initial position of the joint angle when $t=0$

φ_f - final position of the joint angle when $t=t_f$

$\dot{\varphi}(0)$ - initial speed of the joint angle when $t=0$

$\dot{\varphi}(t_f)$ - initial speed of the joint angle when $t=t_f$

$\ddot{\varphi}(0)$ - initial acceleration of the joint angle when $t=0$

$\ddot{\varphi}(t_f)$ - initial acceleration of the joint angle when $t=t_f$

The boundary conditions of the joint are selected based on the designed walking gait. There are three different categories of strides that form a full walking cycle, i.e. starting stride, full stride and ending stride. Furthermore, the postures for each stride are divided into three intermediate positions, i.e. initial position, lift up position and touch down position.

1) Starting stride

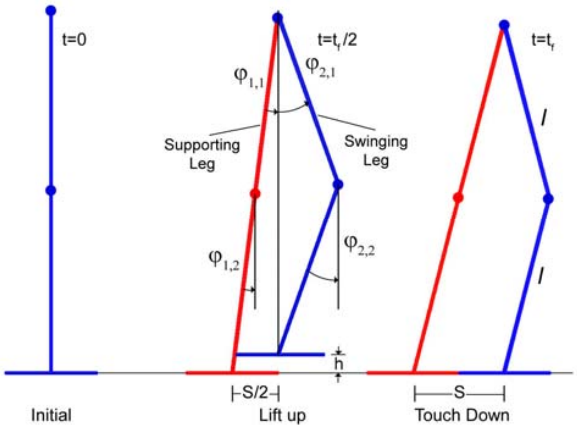

Fig. 2 Leg posture of starting stride

In Fig. 2, $\varphi_{1,1}$ and $\varphi_{1,2}$ are the joint angles for hip and knee joints of the supporting leg respectively, whereas $\varphi_{2,1}$ and $\varphi_{2,2}$ are the joint angles for hip and knee joints of the swinging leg respectively. l is the equal length for both upper and lower legs. It is clear from the drawing that during the first step motion, the supporting leg is responsible for providing a forward step motion S, and the swing leg is responsible for providing a lifting motion for its foot.

The lift up position for the swinging leg is to ensure that the foot will be lifted up by distance h while the robot is taking a aboveground step instead of dragging it along the surface of the ground. The angular boundary conditions for $\varphi_{1,1}$, $\varphi_{1,2}$, $\varphi_{2,1}$ and $\varphi_{2,2}$ can be calculated from the geometry of the leg postures shown in Fig. 2. We assume that full time t_f corresponds to full step size S.

The angular boundary conditions for supporting leg for $0<t<t_f$

$$\varphi_{1,1}(0)=\varphi_{1,2}(0)=0$$

$$\varphi_{1,1}(t_f)=\varphi_{1,2}(t_f)=-\sin^{-1}\left(\frac{S}{2l}\right)$$

The angular boundary conditions for swinging leg

for $0 < t < \frac{t_f}{2}$

$$\varphi_{2,1}(0) = \varphi_{2,2}(0) = 0$$

$$\varphi_{2,1}(\frac{t_f}{2}) = -\varphi_{2,2}(\frac{t_f}{2}) = \cos^{-1}\left(\frac{\sqrt{(2l)^2 - \left(\frac{S}{2}\right)^2} - h}{2l}\right)$$

for $\frac{t_f}{2} < t < t_f$

$$\varphi_{2,1} = -\varphi_{2,2}$$

$$\varphi_{2,1}\left(\frac{t_f}{2}\right) = -\varphi_{2,2}\left(\frac{t_f}{2}\right) = \cos^{-1}\left(\frac{\sqrt{(2l)^2 - \left(\frac{S}{2}\right)^2} - h}{2l}\right)$$

$$\varphi_{2,1}(t_f) = -\varphi_{2,2}(t_f) = \sin^{-1}\left(\frac{S}{2l}\right)$$

2) Full stride

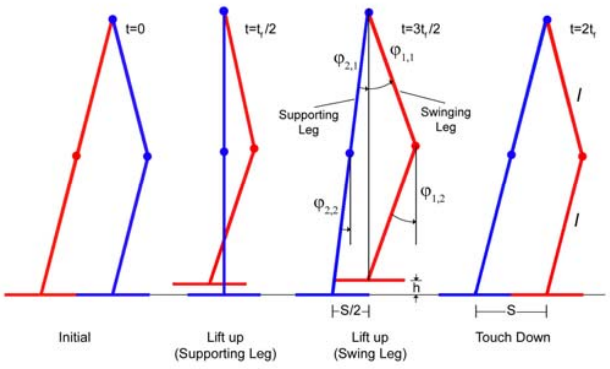

Fig. 3 Leg posture of full stride

In Fig. 3, $\varphi_{1,1}$ and $\varphi_{1,2}$ are joint angles for hip and knee joints of the swinging leg respectively, whereas $\varphi_{2,1}$ and $\varphi_{2,2}$ are the joint angles for hip and knee joints of the supporting leg respectively. The lift up positions for supporting and swinging legs appears at different time. For supporting leg, the lift up position takes place when $t=t_f$ and for swinging leg, the lift up position takes place when $t=(3/2)t_f$.

As shown in Fig. 3, from the initial to lift up position, the supporting leg is stretching and thus provides a lifting up force for the hip. This is important to ensure stability of the robot during the single legged support phase. At lift up position for the swinging leg, the foot of the swinging leg is lifted up by distance h from the ground to provide clearance between the ground and foot during the stride.

The angular boundary conditions for $\varphi_{1,1}$, $\varphi_{1,2}$, $\varphi_{2,1}$ and $\varphi_{2,2}$ can be calculated from the geometry of the leg postures according to Fig. 3. One full stride takes time $2t_f$ and leg advances by distance $2S$.

The angular boundary conditions for swinging leg

for $0 < t < \frac{3t_f}{2}$

$$\varphi_{1,1}(0) = \varphi_{1,2}(0) = -\sin^{-1}\left(\frac{S}{2l}\right)$$

$$\varphi_{1,1}(t_f) = -\varphi_{1,2}(t_f) = \cos^{-1}\left(\frac{\sqrt{(2l)^2 - \left(\frac{S}{2}\right)^2} - h}{2l}\right)$$

for $\frac{3t_f}{2} < t < 2t_f$

$$\varphi_{1,1}(\frac{3t_f}{2}) = \varphi_{1,2}(\frac{3t_f}{2}) = \cos^{-1}\left(\frac{\sqrt{(2l)^2 - \left(\frac{S}{2}\right)^2} - h}{2l}\right)$$

$$\varphi_{1,1}(2t_f) = -\varphi_{1,2}(2t_f) = \sin^{-1}\left(\frac{S}{2l}\right)$$

The angular boundary conditions for supporting leg

for $0 < t < t_f$

$$\varphi_{2,1}(0) = -\varphi_{2,2}(0) = \sin^{-1}\left(\frac{S}{2l}\right)$$

$$\varphi_{2,1}(t_f) = \varphi_{2,2}(t_f) = 0$$

for $t_f < t < 2t_f$

$$\varphi_{2,1}(t_f) = \varphi_{2,2}(t_f) = 0$$

$$\varphi_{2,1}(2t_f) = \varphi_{2,2}(2t_f) = -\sin^{-1}\left(\frac{S}{2l}\right)$$

3) Ending stride

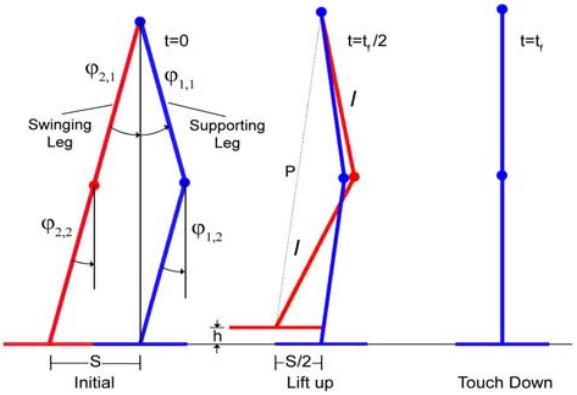

Fig. 4 Leg posture of ending stride

In Fig. 4, $\varphi_{1,1}$ *and* $\varphi_{1,2}$ are the joint angles for hip and knee

joints of the supporting leg respectively, whereas $\varphi_{2,1}$ *and* $\varphi_{2,2}$ are the joint angles for hip and knee joints of the swinging leg respectively.

This step is to end the entire walking cycle by making both legs standing straight up. During this stride, the supporting leg is stretching whereas the swinging leg moves its foot to line up with the supporting foot.

The lift up position for the swinging leg is meant to ensure that the foot will be lifted up by distance *h* above the ground instead of being dragged along the ground surface during the step.

The angular boundary conditions for $\varphi_{1,1}$, $\varphi_{1,2}$, $\varphi_{2,1}$ *and* $\varphi_{2,2}$ can be calculated from the geometry of the leg postures shown in Fig. 4. We assume that full time t_f corresponds to full step size *S*.

The boundary conditions for supporting leg

for $0 < t < t_f$

$$\varphi_{1,1}(0) = -\varphi_{1,2}(0) = \sin^{-1}\left(\frac{S}{2l}\right)$$

$$\varphi_{1,1}(t_f) = \varphi_{1,2}(t_f) = 0$$

The boundary conditions for swinging leg

for $0 < t < \frac{t_f}{2}$

$$\varphi_{2,1}(0) = \varphi_{2,2}(0) = -\sin^{-1}\left(\frac{S}{2l}\right)$$

$$\varphi_{2,1}(\frac{t_f}{2}) = -\left(\sin^{-1}\left(\frac{S/2}{P}\right) - \cos^{-1}\left(\frac{P}{2l}\right)\right)$$

$$\varphi_{2,2}(\frac{t_f}{2}) = -\left(\sin^{-1}\left(\frac{S/2}{P}\right) + \cos^{-1}\left(\frac{P}{2l}\right)\right)$$

for $\frac{t_f}{2} < t < t_f$

$$\varphi_{2,1} = -\varphi_{2,2}$$

$$\varphi_{2,1}(\frac{t_f}{2}) = -\left(\sin^{-1}\left(\frac{S/2}{P}\right) - \cos^{-1}\left(\frac{P}{2l}\right)\right)$$

$$\varphi_{2,2}(\frac{t_f}{2}) = -\left(\sin^{-1}\left(\frac{S/2}{P}\right) + \cos^{-1}\left(\frac{P}{2l}\right)\right)$$

$$\varphi_{2,1}(t_f) = -\varphi_{2,2}(t_f) = \sin^{-1}\left(\frac{S}{2l}\right)$$

where *P* can be calculated as follows :

$$P = \sqrt{\left(2l\cos\left(\frac{\sin^{-1}(S/2l)}{2}\right) - h\right)^2 + \left(\frac{S}{2}\right)^2}$$

B. *Joint space trajectory planning*

Trajectory planning for the postures shown in Fig. 2, 3 and 4 are designed based on linear segment blended with polynomial sections. This type of planning will produce less tension on the actuators because they will run with nominal constant speed most of the time. Secondly, the order of the trajectory curve will be lesser compared to the one using pure polynomial functions.

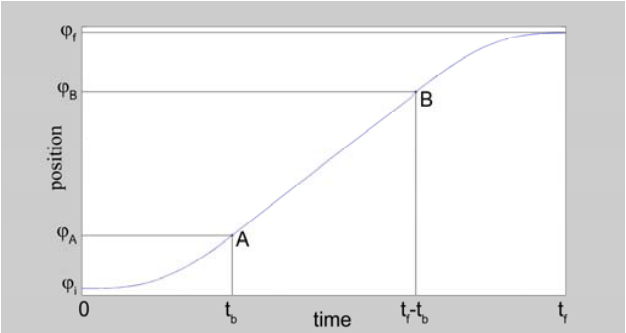

Fig. 5 Linear segment with parabolic blends

Selection of linear segments blended with fourth order polynomial sections will smooth the transition between the postures up to acceleration level.

The angular boundary conditions for the actuator shaft are:

$$\varphi(0) = \varphi_i \;;\; \varphi(t_f) = \varphi_f$$
$$\dot{\varphi}(0) = 0 \;\;;\; \dot{\varphi}(t_f) = 0 \qquad (1)$$
$$\ddot{\varphi}(0) = 0 \;\;;\; \ddot{\varphi}(t_f) = 0$$

The fourth order polynomial and derivatives are as follow:

$$\varphi(t) = c_0 + c_1 t + \frac{1}{2}c_2 t^2 + \frac{1}{3}c_3 t^3 + \frac{1}{4}c_4 t^4$$
$$\dot{\varphi}(t) = c_1 + c_2 t + c_3 t^2 + c_4 t^3$$
$$\ddot{\varphi}(t) = c_2 + 2c_3 t + 3c_4 t^2$$

Substituting the initial boundary condition (1) to the polynomial gives:

$$\varphi(t) = \varphi_i + \frac{1}{3}c_3 t^3 + \frac{1}{4}c_4 t^4$$
$$\dot{\varphi}(t) = c_3 t^2 + c_4 t^3$$
$$\ddot{\varphi}(t) = 2c_3 t + 3c_4 t^2$$

Fig. 5 shows angular motion of the actuator designed as linear segment blended with polynomial sections at the beginning and the end of the motion period.

Matching the first and second derivatives of the polynomial with constant speed ω and zero acceleration to the linear segment of the trajectory yields the following expression:

$$\dot{\varphi}_A = c_3 {t_b}^2 + c_4 {t_b}^3 = \omega$$
$$\ddot{\varphi}_A = 2c_3 t_b + 3c_4 {t_b}^2 = 0 \qquad (2)$$

Solving equations (2) simultaneously yields:

$$c_3 = \frac{3\omega}{t_b^{\,2}} \quad ; \quad c_4 = -\frac{2\omega}{t_b^{\,3}}$$

Matching the boundary angular values for polynomial and linear segments yields:

$$\varphi_A = \varphi_i + \frac{1}{3}c_3 t_b^{\,3} + \frac{1}{4}c_4 t_b^{\,4} \;\; ; \;\; \varphi_B = \varphi_A + \omega(t_f - 2t_b)$$

$$\varphi_f = \varphi_B + (\varphi_A - \varphi_i)$$

$$\varphi_f = \varphi_A + \omega(t_f - 2t_b) + (\varphi_A - \varphi_i)$$

$$\varphi_f = 2\varphi_A - \varphi_i + \omega(t_f - 2t_b)$$

$$\varphi_f = 2\left(\varphi_i + \frac{1}{3}c_3 t_b^{\,3} + \frac{1}{4}c_4 t_b^{\,4}\right) - \varphi_i + \omega t_f - 2\omega t_b$$

$$\varphi_f = 2\varphi_i + \frac{2}{3}c_3 t_b^{\,3} + \frac{1}{2}c_4 t_b^{\,4} - \varphi_i + \omega t_f - 2\omega t_b$$

$$\varphi_f = 2\varphi_i + \frac{2}{3}\left(\frac{3\omega}{t_b^{\,2}}\right)t_b^{\,3} + \frac{1}{2}\left(-\frac{2\omega}{t_b^{\,3}}\right)t_b^{\,4} - \varphi_i + \omega t_f - 2\omega t_b$$

$$\varphi_f = 2\varphi_i + 2\omega t_b + \omega t_b - \varphi_i + \omega t_f - 2\omega t_b$$

$$t_b = \frac{\varphi_i - \varphi_f + \omega t_f}{\omega}$$

The motion of the actuator for three separate time segments can be expressed as:

for $0 < t \le t_b$

$$\varphi(t) = \varphi_i + \left(\frac{\omega}{t_b^{\,2}}\right)t^3 + \frac{1}{2}\left(\frac{\omega}{t_b^{\,3}}\right)t^4$$

$$\dot{\varphi}(t) = \left(\frac{3\omega}{t_b^{\,2}}\right)t^2 - \left(\frac{2\omega}{t_b^{\,3}}\right)t^3$$

$$\ddot{\varphi}(t) = \left(\frac{6\omega}{t_b^{\,2}}\right)t - \left(\frac{6\omega}{t_b^{\,3}}\right)t^2$$

for $t_A < t \le t_B$

$$\varphi(t) = \varphi_A + \omega t$$

$$\dot{\varphi}(t) = \omega$$

$$\ddot{\varphi}(t) = 0$$

for $t_B < t \le t_f$

$$\varphi(t) = \varphi_f - \left(\frac{\omega}{t_b^{\,2}}\right)(t_f - t)^3 + \frac{1}{2}\left(\frac{\omega}{t_b^{\,3}}\right)(t_f - t)^4$$

$$\dot{\varphi}(t) = \left(\frac{3\omega}{t_b^{\,2}}\right)(t_f - t)^2 - \left(\frac{2\omega}{t_b^{\,3}}\right)(t_f - t)^3$$

$$\ddot{\varphi}(t) = -\left(\frac{6\omega}{t_b^{\,2}}\right)(t_f - t) + \left(\frac{6\omega}{t_b^{\,3}}\right)(t_f - t)^2$$

IV. Simulation of The Bipedal Motion Trajectories

To simulate the bipedal motion, arbitrary step size *S*, leg lifting height *h*, leg length *l* and time interval for full step t_f are selected. The simulation according to the postures selected in Fig. 2, 3 and 4 yields the strides shown in Fig. 6.

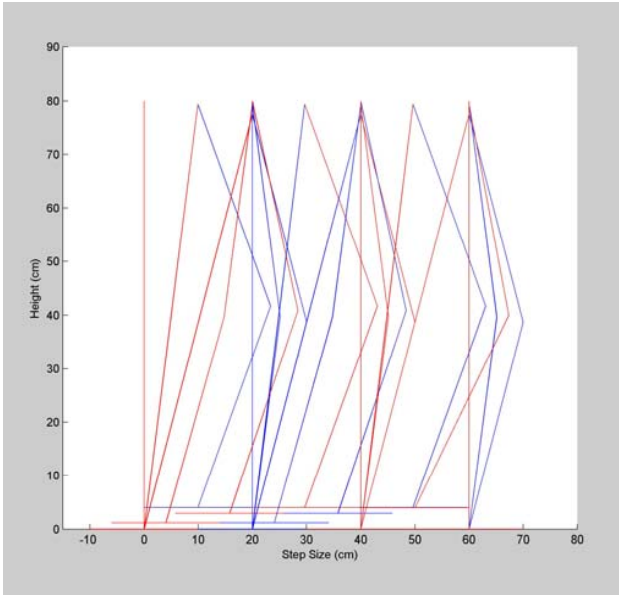

Fig. 6 Stick diagram for walking pattern

Fig. 7, 8 and 9 show the position, velocity and acceleration for each joint of the leg 1 and 2 during the simulated walk. From the figures it is clear that the target of providing a smooth transition between the strides has been achieved up to the second order derivatives of the motion characteristics.

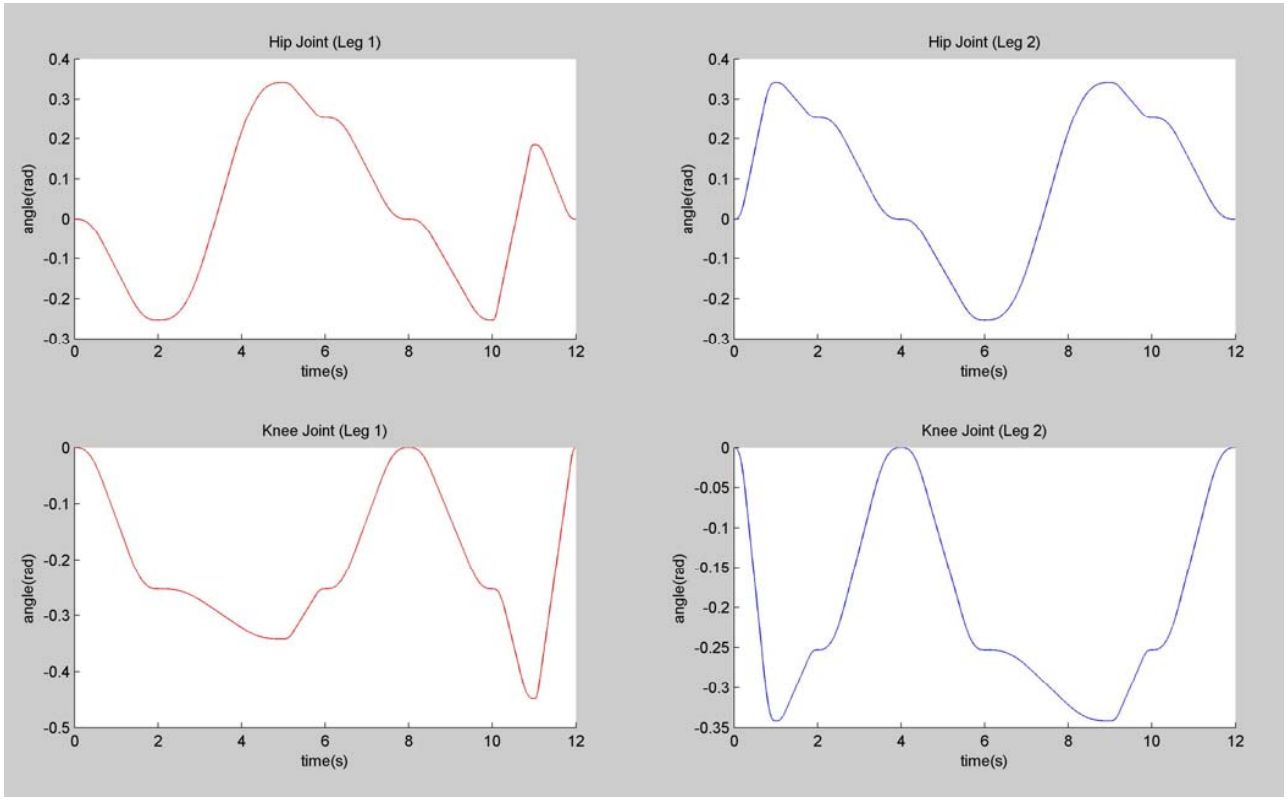

Fig. 7 Joint position during walking

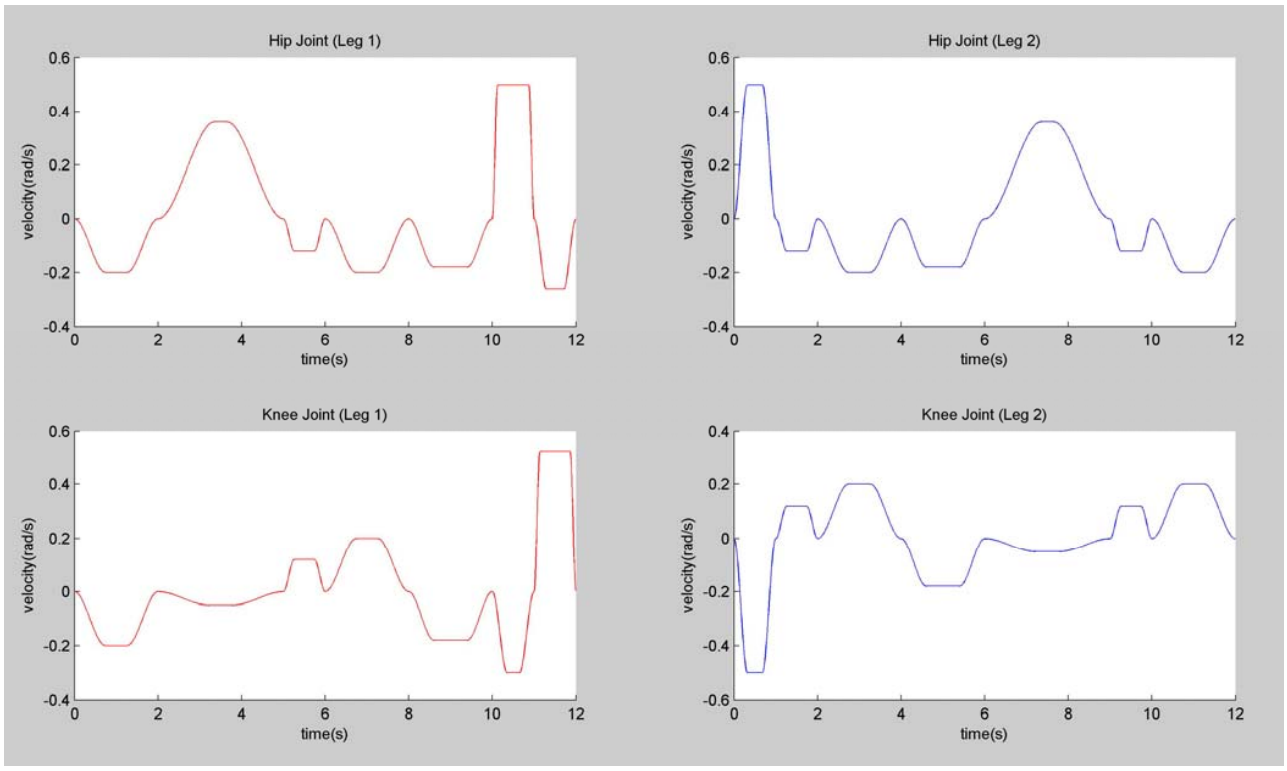

Fig. 8 Joint velocity during walking

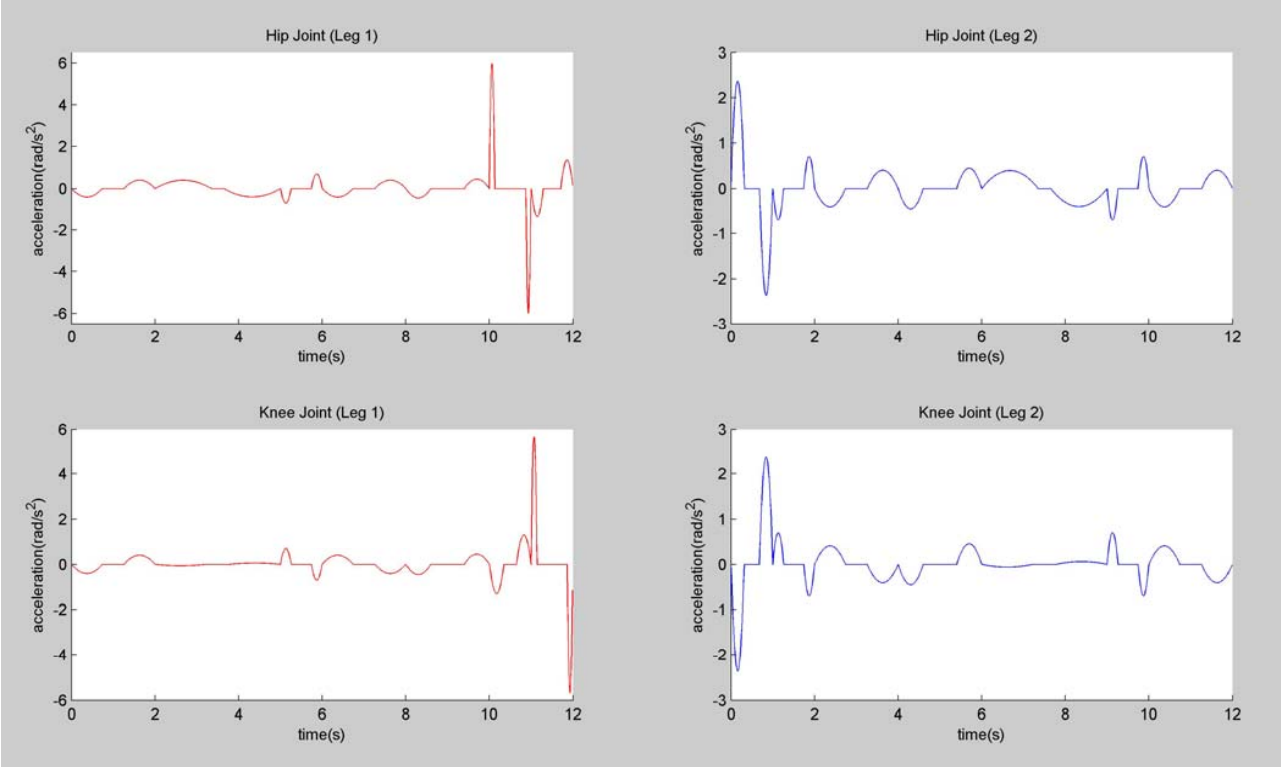

Fig. 9 Joint acceleration during walking

V. Conclusion

The paper describes the new type of bipedal walking robot which requires a minimum number of actuations yet lightweight and energy efficient. A novel approach of implementing joint coordinate trajectory planning is also presented as an alternative to realize straight legged walking which cannot be achieved by conventional inverse kinematics trajectory planning. The results of computer simulation demonstrate that the planned trajectories are within an applicable range for all four actuators limits while the walking robot demonstrates smooth legs motion (Fig. 7, 8, 9).

References

[1] C. Chevallereau and P. Sardain, "Design and Actuation Optimization of a 4 axes Biped Robot for Walking and Running," in *Proc. IEEE Int. Conf on Robotics and Automation*, San Francisco, 2000, pp. 3365–3370.

[2] M. Guihard and P. Gorce, *"Dynamic Control of Bipeds Using Ankle and Hip Strategies,"* in *Proc. IEEE/RSJ Int. Conf. on Intelligent Robots and Systems*, Lausanne, 2002, pp. 2587–2592.

[3] H. Wongsuwarn and D. Laowattana, *"Experimental Study for a FIBO Humanoid Robot,"* in *Proc. IEEE Int. Conf. on Robotics, Automation and Mechatronics*, Bangkok, 2006, pp. 1–6.

[4] K. Y. Yi, *"Locomotion of Biped Robot with Compliant Ankle Joint,"* in *Proc. IEEE Int. Conf. on Robotics and Automation*, New Mexico, 1997, pp. 199–204.

[5] K. Loffler, M. Gienger and F. Pfeiffer, *"Sensor and Control Design of a Dynamically Stable Biped Robot,"* in *Proc. IEEE Int. Conf. on Robotics, Automation and Mechatronics*, Taipei, 2003, pp. 484–490.

[6] K. Hirai, M. Hirose, Y. Haikawa and T. Takenaka, *"The Development of Honda Humanoid Robot,"* in *Proc. IEEE Int. Conf. on Robotics, Automation and Mechatronics*, Leuven, 1998, pp. 1321–1326.

[7] Y. Sakagami, R. Watanabe, C. Aoyama, S. Matsunaga, N. Higaki and K. Fujimura, *"The Intelligent ASIMO: System Overview and Integration,"* in *Proc. IEEE Int. Conf. on Intelligent Robots and Systems*, Lausanne, 2002, pp. 2478–2483.

[8] J. Yamaguchi, A. Takanishi, and I. Kato, *"Development of a Biped Walking Robot Compensating for Three-Axis Moment by Trunk Motion,"* in *Proc. IEEE Int. Conf. on Intelligent Robots and Systems*, Yokohama, 1993, pp. 561–566.

[9] J. Yamaguchi, E. Soga, S. Inoue and A. Takanishi, *"Development of a Bipedal Humanoid Robot Control Method of Whole Body Cooperative Dynamic Biped Walking,"* in *Proc. IEEE Int. Conf. Robotics and Automation*, Michigan, 1999, pp. 368–374.

[10] Q. Li, A. Takanishi and I. Kato, *"A Biped Walking Robot Having A ZMP Measurement System Using Universal Force-Moment Sensors,"* in *Proc. IEEE/RSJ Int. Workshop on Intelligent Robots and Systems*, Osaka, 1991, pp. 1568–1573.

[11] R. Kurazume, S. Tanaka and M. Yamashita, *"Straight Legged Walking of a Biped Robot,"* in *Proc. IEEE/RSJ Int. Conf. on Intelligent Robots and Systems*, Alberta, 2005, pp. 3095–3101.

[12] Y. Ogura, H. Lim and A. Takanishi, *"Stretch Walking Pattern Generation for a Biped Humanoid Robot,"* in *Proc. IEEE/RSJ Int. Workshop on Intelligent Robots and Systems*, Nevada, 2003, pp. 352–357.